A Numerical Simulation of Nonadiabatic Electron Excitation in the Strong Field Regime: Linear Polyenes

Stanley M. Smith,[†] Xiaosong Li,[‡] Alexei N. Markevitch,[§] Dmitri A. Romanov,[⊥] Robert J. Levis,[§] and H. Bernhard Schlegel*,[†]

Department of Chemistry, Wayne State University, Detroit, Michigan 48202, Department of Chemistry, Yale University, New Haven, Connecticut 06520, and Department of Chemistry and Department of Physics, Center for Advanced Photonics Research, Temple University, Philadelphia, Pennsylvania 19122

Received: February 24, 2005; In Final Form: April 19, 2005

Time-dependent Hartree−Fock theory has been used to study of the electronic optical response of a series of linear polyenes in strong laser fields. Ethylene, butadiene, and hexatriene have been calculated with 6-31G(d,p) in the presence of a field corresponding to 8.75×10^{13} W/cm^2 and 760 nm. Time evolution of the electron population indicates not only the π electrons, but also lower lying valence electrons are involved in electronic response. When the field is aligned with the long axis of the molecule, Löwdin population analysis shows large charges at each end of the molecule. For ethylene, the instantaneous dipole moment followed the field adiabatically, but for hexatriene, nonadiabatic effects were very pronounced. For constant intensity, the nonadiabatic effects in the charge distribution, instantaneous dipole, and orbital populations increased nonlinearly with the length of the polyene. These calculations elucidate the mechanism of the strong field nonadiabatic electron excitation of polyatomic molecules leading to their eventual ionization and fragmentation. The described computational methods are a viable tool for studying the complex processes in multielectron atomic and molecular systems in strong laser fields.

I. Introduction

Intense femtosecond and picosecond lasers are able to produce electric fields that are comparable to the potentials of valence electrons. This leads to a variety of phenomena known as strong-field effects. They include Coulomb explosions,[1−4] above threshold ionization[5,6] and dissociation,[7−13] generation of higher-order harmonic emissions,[14−18] bond softening and hardening,[19−22] charge-resonance-enhanced ionization,[23,24] nonadiabatic multielectron dynamics (NMED),[25−28] and nonadiabatic charge localization.[4] Understanding the response of the electronic wave function to strong fields is essential for description of these phenomena, particularly in polyatomic molecules.

When the above-mentioned processes are studied in strong fields with an emphasis on polyatomic molecules, conjugated hydrocarbons are frequently used as models. Specifically, intense field dissociation and ionization processes have been reported for conjugated polyatomic molecules such as benzene, naphthalene, anthracene, hexatriene, decatetraene, octatetraene, and C_{60}.[25−35] A number of analytical models have been proposed, in which various molecular properties can help predict the outcome of the laser molecule interaction. In the adiabatic regime, the coupling of the molecules to the laser field is mainly determined by transition dipole matrix elements and first-order polarizability. Higher order contributions are governed by the hyperpolarizabilities. These properties have been extensively studied for conjugated systems, particularly linear polyenes.[36−46] Since polarizabilities and hyperpolarizabilities increase nonlinearly with increasing length and conjugation, longer polyenes should exhibit larger oscillator strength than the shorter polyenes. At high intensities, electrons can be excited nonadiabatically through multiphoton and nonadiabatic multielectron dynamic processes.[25−28] In the present work we use time-dependent Hartree−Fock theory to probe these multielectron and nonadiabatic processes in linear conjugated hydrocarbons.

In a high-intensity laser field, the electronic dynamics can no longer be described by perturbative calculations.[47−49] For one- and two-electron systems, it is feasible to perform numerical integrations of the full time-dependent Schrödinger equation (TDSE).[50−52] However, for many electron systems, some approximations must be made. The time-dependent Hartree−Fock (TDHF) method is widely used to treat the interaction of a molecule and light.[53−58] Because it avoids the explicit computation of the excited states, TDHF is much less demanding than multiple configuration self-consistent field (MCSCF) based algorithms.

Charge redistribution and bond softening and hardening have been studied computationally by using time-dependent Hartree−Fock with the Parser−Parr−Pople (PPP) Hamiltonian in the nonionizing[19] regime while ionization saturation intensities[59] have been studied by using time-dependent Hartree−Fock in one-dimensional potentials. As expected, for octatetraene subjected to nonionizing electric field pulses of approximately 50 fs in duration, there is charge transfer between nearest neighbor atoms. It is found that the charge fluctuation no longer follows the field adiabatically as the field strength is systematically increased. The bond order oscillates with the field, indicating a periodic variation in the bond length associated with the bond length alternation models for octatetraene and decatetraene subjected to a high-intensity field, and exhibits ionization behavior similar to experimental results.[59] The ionization saturation intensity for decatetraene is similar to the experi-

[†] Wayne State University.
[‡] Yale University.
[§] Department of Chemistry, Center for Advanced Photonics Research.
[⊥] Department of Physics, Center for Advanced Photonics Research.

10.1021/jp050968n CCC: $30.25
Published on Web 05/18/2005

mentally reported value.[26] This method successfully captures some of the experimental results; however, the model Hamiltonian treats only the π electrons. Previous calculations[58] indicate that Coulombic interactions between electrons, electron correlation, and excitation of σ valence electrons may also contribute to the experimentally observed nonadiabatic processes

The full time-dependent Hartree−Fock method[58] has recently been used for all electron simulations of some diatomics in intense laser fields. For a short pulse of ca. 7 fs in the nonionizing regime, the dipole moment and charge distribution of H_2 and N_2 do not always follow the field adiabatically. For a continuous wave (CW) excitation with a maximum field intensity of 1.72×10^{14} W/cm^2, population of the S_2 state is observed for H_2 even though the $S_0 \rightarrow S_2$ transition is forbidden. The population of the S_2 state appears to come from sequential $S_0 \rightarrow S_1$ and $S_1 \rightarrow S_2$ transitions. The time evolution of the orbital energies, orbital occupations numbers, and instantaneous dipole moments can be readily determined by TDHF calculations and help to describe electron dynamics in polyatomic molecules.

The goal of this paper is to follow the electron dynamics for ethylene, butadiene, and hexatriene in intense laser fields prior to ionization. These simple linear polyenes comprise a series in which the number of active electrons, the electron delocalization, and the polarizability increase systematically with molecular size. For suitably chosen laser field conditions, the nonresonant electronic response of these molecules should range from adiabatic to nonadiabatic. The conditions selected for this study are $\mathbf{E}_{max} = 0.05$ au and $\omega = 0.06$ au, corresponding to an intensity of 8.75×10^{13} W/cm^2. The experimental values of saturation intensity vary for the hexatriene range from 5×10^{13} (ref 26) to 8.9×10^{13} W/cm^2 (refs 60 and 61) for ca. 800 nm electric fields. These saturation intensities were measured by using laser pulses of ca. 44 fs duration. In our calculations we apply the electric field for a much shorter time of ~7 fs. Thus, significant ionization is not expected to occur during the laser pulse, and the chosen conditions allow us to discuss the observed trends as occurring prior to ionization.

II. Methodology

In the time-dependent Hartree−Fock (TDHF)[58] method, the wave function is represented by a single Slater determinant of one-electron orbitals that are a function of time.

$$\psi(t) = A[\phi_1(t)\phi_2(t)...\phi_i(t)] \tag{1}$$

The molecular orbitals can be expanded in terms of basis functions χ_μ and time dependent molecular orbital coefficients $c_{\mu,i}(t)$,

$$\phi_i(t) = \sum_\mu c_{\mu,i}(t)\chi_\mu \tag{2}$$

The one-electron density matrix is given by the product of the molecular orbital coefficients

$$P'_{\mu\nu}(t) = \sum_i^{occ} n_i\, c^*_{\mu,i}(t) \cdot c_{\nu,i}(t) \tag{3}$$

where n_i are the occupation numbers. In an orthonormal basis, the TDHF equations can be written in terms of the Fock matrix and the density matrix,

$$i\frac{d\mathbf{P}(t_i)}{dt} = [\mathbf{F}(t_i),\mathbf{P}(t_i)] \tag{4}$$

In general, the atomic orbital (AO) basis functions are not orthonormal; hence, the overlap matrix

$$\mathbf{S}_{\mu\nu} = \langle\chi_\mu|\chi_\nu\rangle \tag{5}$$

is not the identity. However, this basis can always be orthonormalized by means of Löwdin or Cholesky transformation methods. The density matrix and the Fock matrix are transformed from the AO basis ($\mathbf{P}'$ and $\mathbf{F}'$) into an orthonormal basis ($\mathbf{P}$ and $\mathbf{F}$) by a transformation matrix $\mathbf{V}$:

$$\mathbf{P} = \mathbf{V}\,\mathbf{P}'\,\mathbf{V}^T \text{ and } \mathbf{F} = \mathbf{V}^{-T}\,\mathbf{F}'\,\mathbf{V}^{-1} \tag{6}$$

In the present work, we use the Löwdin orthonormalization method, $\mathbf{V} = \mathbf{S}^{1/2}$. Alternatively, an upper triangular $\mathbf{V}$ can be obtained by the Cholesky decomposition, $\mathbf{S} = \mathbf{V}^T\mathbf{V}$.

The Fock matrix depends on the density and the external field. For molecules interacting with linearly polarized light, to a good approximation, the electric field is given by

$$\mathbf{e}(t_i) \approx \mathbf{E}(t_i)\sin(\omega t_i + \varphi) \tag{7}$$

The time dependent Fock matrix can then be written in terms of the field-free Fock matrix, $\mathbf{F}_0(t)$, and the dipole moment integrals, $\mathbf{D}_{ij} = \langle\varphi_i|\mathbf{r}|\varphi_j\rangle$

$$\mathbf{F}(t) = \mathbf{F}_0(t) + \mathbf{D}\cdot\mathbf{e}(t) \tag{8}$$

Note that the field-free Fock matrix depends on time because the density matrix is time dependent.

Two temporal field profiles were used for this study. For a continuous wave (CW) profile, the field envelop $|\mathbf{E}(t)|$ is ramped up linearly from zero to $|\mathbf{E}_{max}|$ at the end of the first cycle and thereafter remains at $|\mathbf{E}_{max}|$.

$$\begin{aligned} &\mathbf{E}(t) = (\omega t/2\pi)\mathbf{E}_{max} && \text{for } 0 \le t \le 2\pi/\omega \\ &\mathbf{E}_{max} && \text{for } t > 2\pi/\omega \end{aligned} \tag{9}$$

To simulate a short pulse, $|\mathbf{E}(t)|$ is increased linearly to $|\mathbf{E}_{max}|$ at the end of the first cycle and remains at $|\mathbf{E}_{max}|$ for one cycle then decreases linearly to zero by the end of the next cycle.

$$\begin{aligned} &\mathbf{E}(t) = (\omega t/2\pi)\mathbf{E}_{max} && \text{for } 0 \le t \le 2\pi/\omega \\ &\mathbf{E}(t) = \mathbf{E}_{max} && \text{for } 2\pi/\omega \le t \le 4\pi/\omega \\ &\mathbf{E}(t) = (3 - \omega t/2\pi)\mathbf{E}_{max} && \text{for } 4\pi/\omega \le t \le 6\pi/\omega \\ &\mathbf{E}(t) = 0 && \text{for } t < 0 \text{ and } t > 6\pi/\omega \end{aligned} \tag{10}$$

For a constant Fock matrix, the TDHF equations can be integrated analytically by using a unitary transformation,

$$\mathbf{P}(t_i + \Delta t) = \mathbf{U}\mathbf{P}(t_i)\mathbf{U}^\dagger = \exp(i\Delta t\mathbf{F})\mathbf{P}(t_i)\exp(-i\Delta t\mathbf{F}) \tag{11}$$

The unitary transform matrix $\mathbf{U}$ can be written in terms of the eigenvectors $\mathbf{C}$ and the eigenvalues ϵ of the Fock matrix:

$$\mathbf{C}^\dagger\,\mathbf{F}\,\mathbf{C} = \epsilon;\ \mathbf{U} = \exp(i\Delta t\mathbf{F}) = \mathbf{C}\exp(i\Delta t\epsilon)\,\mathbf{C}^\dagger \tag{12}$$

Since the matrix $\mathbf{U}$ is unitary, the idempotency constraint is preserved automatically for any size of time step. However, the Fock matrix changes during the time step both because of the external field and because of the time dependence of the density matrix. To take into account linear changes in the Fock matrix, the unitary transformation is computed by using $\mathbf{F}(t)$ at the

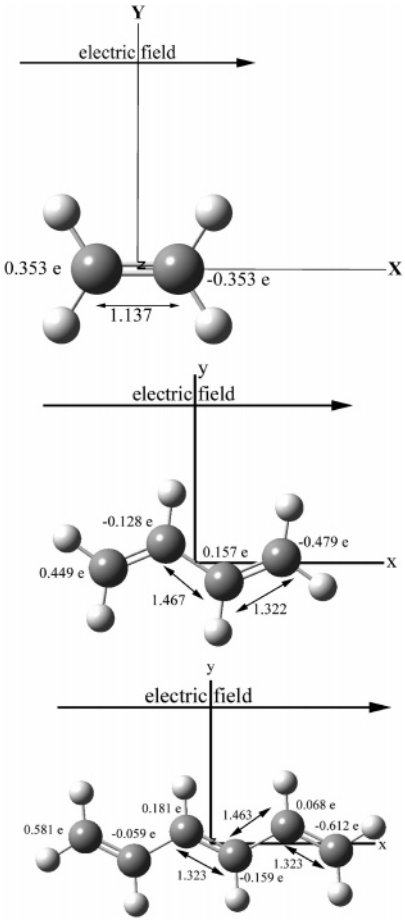

Figure 1. Ground state of ethylene, butadiene, and hextriene computed at HF/6-31G(d,p), showing optimized bond lengths in the absence of a field and Löwdin charges on the CH and CH_2 groups in the presence of a 0.05 au field applied along the *x* axis.

midpoint of the time step. This corresponds to a modified midpoint algorithm along with the unitary transform method for integrating the TDHF equations (MMUT-TDHF).

$$\mathbf{U} = \exp(2i\Delta t\mathbf{F}(t_i)) \text{ and } \mathbf{P}(t_{i+1}) = \mathbf{U}\,\mathbf{P}(t_{i-1})\,\mathbf{U}^{\dagger} \quad (13)$$

This approach was developed and tested in our previous paper,[58] and is comparable to Micha's "relax and drive" method.[62,63]

To characterize the behavior of a molecule in an intense field, several properties are useful. The effective charge on atom α can be computed by using the Löwdin population analysis,

$$q_\alpha = Z_\alpha - \sum_{i\subset\alpha} P_{ii}(t) \quad (14)$$

where Z_α is the charge on the nucleus, P_{ii} are the diagonal elements of the density matrix in the orthonormal basis, and the sum is over basis functions on atom α. Orbital occupation numbers are obtained by projecting the time-dependent density matrix onto the initial, field-free orbitals

$$n_k(t_i) = \mathbf{C}_k^{\mathrm{T}}(0)\,\mathbf{P}(t_i)\,\mathbf{C}_k(0) \quad (15)$$

where $\mathbf{C}_k(0)$ is the *k*th eigenvector of the converged Fock matrix at $t = 0$. The instantaneous dipole moment is given by

$$\mu(t_i) = \sum_\alpha Z_\alpha \mathbf{R}_\alpha - tr(\mathbf{D}'\mathbf{P}'(t_i)) \quad (16)$$

where $\mathbf{D}'$ are the dipole moment integrals in the AO basis. For

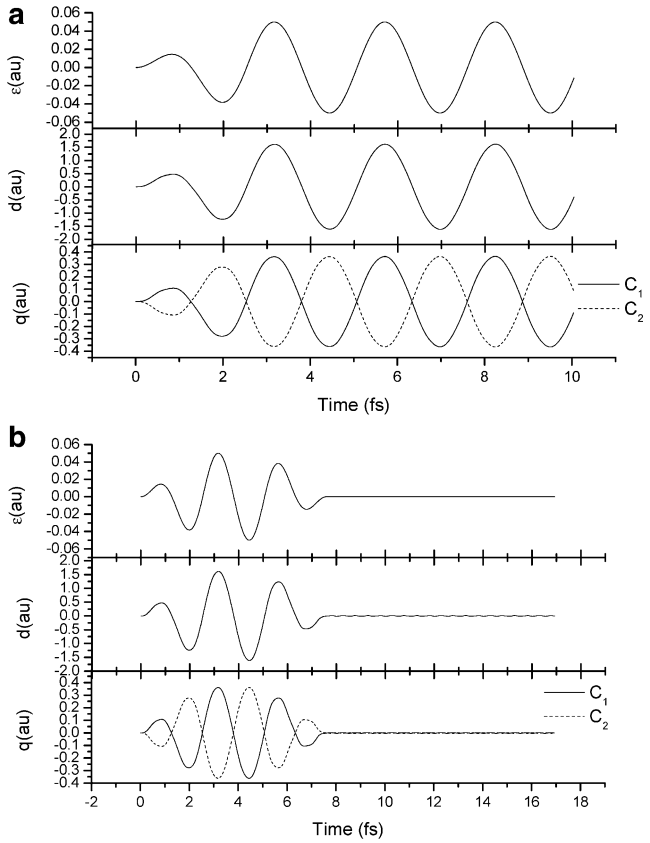

Figure 2. Time evolution of the electric field, instantaneous dipole, and charge distribution of ethylene in CW and pulsed fields (TDHF/6-31G(d,p), $\mathbf{E}_{max} = 0.05$ au (3.5×10^{14} W/cm^2) and $\omega = 0.06$ au (760 nm)).

TABLE 1: Lowest Four Excited States of Ethylene with Oscillator Strength Greater than 0.01 Computed with Linearized TDHF/6-31G(d,p)

excited states	electron transitions (coefficients)	excitation energy in eV (wavelength in nm)	oscillator strength
1^1B_u	HOMO → LUMO (0.65)	8.2511 (150.26)	0.4506
2^1B_u	HOMO−3 → LUMO+4 (−0.12)	14.4996 (85.51)	0.7338
	HOMO−1 → LUMO+2 (0.67)		
3^1B_u	HOMO−3 → LUMO+1 (0.25)	14.7670 (83.96)	1.0704
	HOMO−1 → LUMO+3 (0.62)		
4^1B_u	HOMO−2 → LUMO+1 (0.12)	15.8627 (78.16)	0.1022
	HOMO−2 → LUMO+2 (0.66)		
	HOMO−1 → LUMO+5 (−0.13)		

the purpose of analysis, it is also useful to write the components of the dipole in terms of the polarizability and the hyperpolarizabilities:

$$\mu_i = \mu_i^0 + \sum_j \alpha_{ij}E_j + \frac{1}{2}\sum_{jk}\beta_{ijk}E_jE_k + \frac{1}{6}\sum_{jkl}\gamma_{ijkl}E_jE_kE_l + \ldots \quad (17)$$

Note that by symmetry the β's do not contribute for the polyenes in the present study.

Electronic dynamics in a field are simulated by using the development version of the Gaussian series of programs[64] with the addition of the modified midpoint unitary transform time-dependent Hartree−Fock algorithm (MMUT-TDHF).[58] Calculations have been performed at the HF/6-31G(d,p) level of theory with a step size of 0.0012 fs. For each of the molecules, the integrations are carried out for 10 fs for CW fields and for 16 fs for pulsed fields. Field parameters are $|\mathbf{E}_{max}| = 0.05$ au (8.75

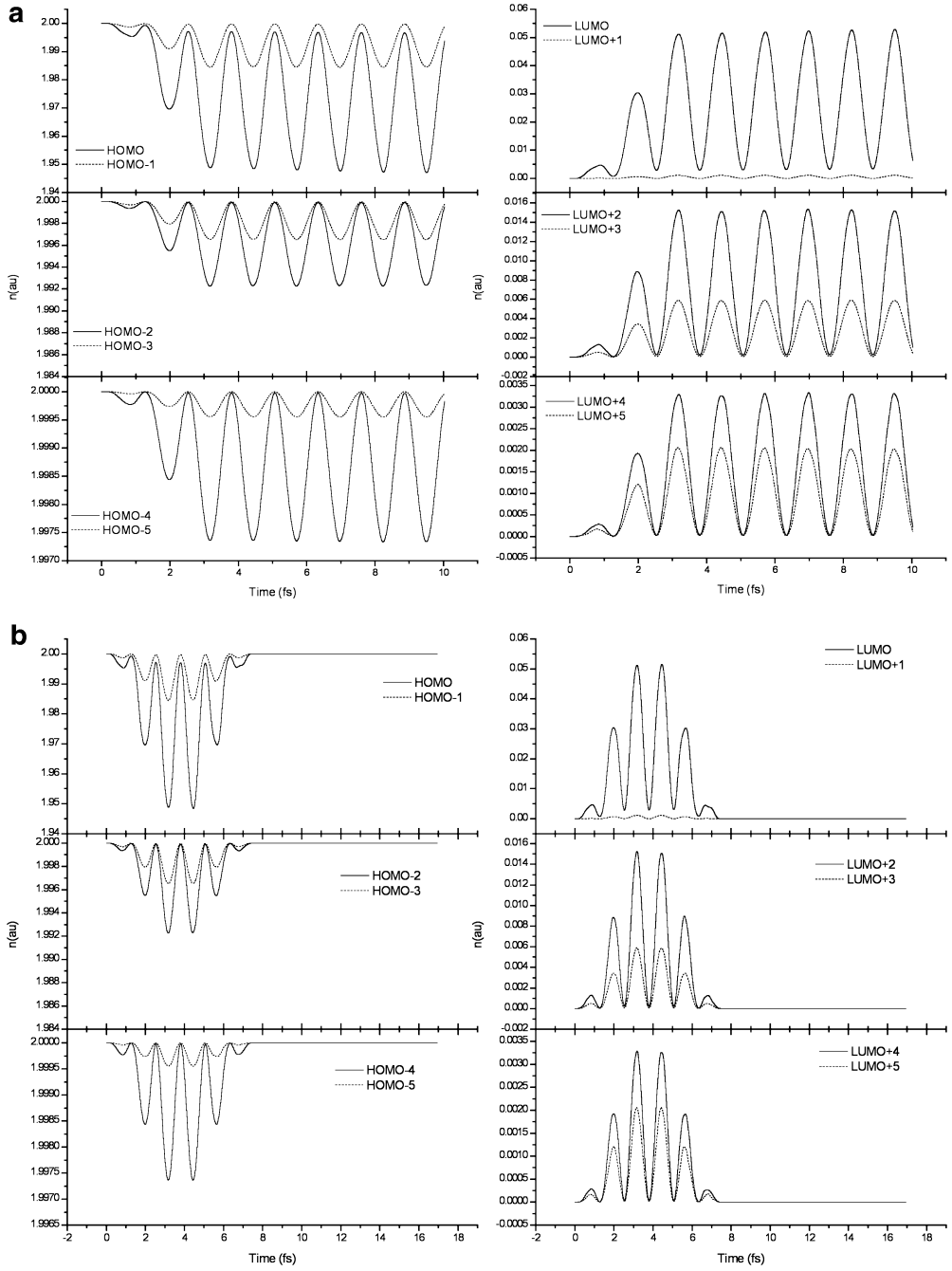

Figure 3. Time evolution of the electron population of the frontier orbitals of ethylene in CW and pulsed fields (TDHF/6-31G(d,p), $\mathbf{E}_{max} = 0.05$ au (3.5×10^{14} W/cm^2) and $\omega = 0.06$ au (760 nm)).

$\times 10^{13}$ W/cm^2) and $\omega = 0.06$ au (760 nm). The initial conditions were equilibrium geometries and the converged ground electronic state. The phase of the field φ is chosen to be zero and the nuclei are not permitted to move.

III. Results and Discussion

As a first step to understanding the interaction of conjugated molecules with strong fields, we have carried out TDHF simulations under the nonionizing conditions. Subsequent studies of processes such as fragmentation and ionization will require more sophisticated methods. In the nonionizing regime, there are a number of properties that can be used to probe the interaction of strong fields with small molecules. In particular, we have examined the dynamic response of the instantaneous dipole, the charge distribution, and orbital occupations with respect to the electric field at a frequency corresponding to the commonly employed Ti:sapphire laser. The response for each of these properties is analyzed for a CW and a pulsed laser (the laser pulse lasts ca. 7 fs). Three linear polyenes—ethylene, butadiene, and hexatriene—are investigated to determine how π delocalization and conjugation effect nonadiabatic interactions with strong fields as molecular size increases. The ground-state geometries, orientations with respect to the applied field, and charge distributions in a static field are shown in Figure 1.

A. Ethylene. The top panels of Figure 2a,b show the time evolution of the CW and pulsed laser fields applied along the C═C axis of ethylene. The middle and bottom panels of Figure 2a,b show the time evolution of the dipole moment and Löwdin charges in response to these fields. While the external field is present, the instantaneous dipole and the charges follow the field adiabatically. For the CW field, the maximum in the instantaneous dipole moment is 1.613 au. The dynamic polarizability

calculated at the HF/6-31G(d,p) level of theory is 32.127 au at $\omega = 0.06$ au. With a field of 0.05 au, this yields a dipole of 1.606 au via eq 17. The excellent agreement with the TDHF simulations indicates that higher order, nonlinear processes are not important for ethylene at this field strength.

The CW field induces charges of ± 0.361 electron on the CH_2 groups. This is slightly larger that the charges produced by a static field of the same magnitude (0.353 electron for a field of 0.05 au, Figure 1). The CW and pulsed fields of the same intensity induce almost identical dipole and charge separation. This confirms that the response of the electrons to the applied field is almost adiabatic under the conditions studied.

For the pulsed field, however, there are some minor residual oscillations in the instantaneous dipole moment and the charges after the field has returned to zero. This indicates that the pulse has produced a small degree of electronic excitation. Table 1 shows that the energy of the lowest excited state is 8.75 eV, calculated at the linearized TDHF/6-31G(d,p) level of theory (also known as the random phase approximation, RPA[65−67]). Since the frequency of the electric field corresponds to an energy of 1.55 eV, this excitation must correspond to a nonadiabatic process.

The orbitals most susceptible to perturbation by an external field are the highest occupied and lowest unoccupied molecular orbitals (HOMO and LUMO). For ethylene, these are the π bonding and the π^* antibonding orbitals. However, the C−H and C−C σ and σ^* orbitals are also affected by the field. A qualitative indication of the most important orbitals can be obtained by looking at the lowest excited state that has significant transition dipoles aligned with the field. Table 1 lists the four excited states whose oscillator strengths are greater than 0.01 calculated at TDHF/6-31G(d,p). The TDHF coefficients show that the field may affect not only the HOMO and LUMO but also HOMO−1 and −2 and LUMO+1, +2, and +3.

Panels a and b of Figure 3 show the time evolution of the electron distribution in terms of the occupation numbers of the MOs of the field-free ground state for the CW and pulsed fields, respectively. The changes in the HOMO and LUMO (π and π^*) are the largest and correspond to $1^1A_g \leftrightarrow 1^1B_u$ excitation and relaxation. The next three excited states with significant intensity are 6−7 eV higher than the $\pi \rightarrow \pi^*$ transition and involve σ and σ^* orbitals HOMO−1, HOMO−2, LUMO+2, and LUMO+3. The oscillations in the populations of these orbitals are a factor of 5−10 smaller than those for the HOMO and LUMO. As in the case with the instantaneous dipole and the charge separation, the pulsed and CW fields of the same intensity produce the same amount of population/depopulation of the frontier orbitals. The observed effects for the σ-type orbitals are not seen in simulations with the PPP Hamiltonian,[19] which treats only the π electrons.

B. Butadiene. The orientation of butadiene in the field is shown in Figure 1 and the response of the charge distribution is presented in Figure 4. As in the case of ethylene, the dipole and the charges appear to follow the field adiabatically. However, closer inspection of the charges on the central atoms reveals a bit of nonadiabatic behavior. The maximum magnitude of the instantaneous dipole is 4.187 au in the TDHF simulations with the CW field. This can be compared to 4.085 au calculated from the dynamic polarizability under the same conditions. The somewhat larger difference (2.1% vs 0.43% in ethylene) indicates that contributions from γ in eq 17 are starting to become noticeable.

A static field of 0.05 au directed along the long axis induces charges 0.449, −0.128, 0.158, and −0.479 on C_1, C_2, C_3, and C_4, respectively (charges on the hydrogens are summed into the carbons). This can be understood in terms of two effects: polarization of the individual π bonds and charge transfer between the π bonds. Alternatively, a simple Hückel model yields the same trend. The maximum charge separation in the dynamic field follows the same pattern: 0.484, −0.127, 0.154, and −0.511 on C_1, C_2, C_3, and C_4, respectively. As can be anticipated from the difference between the dynamic and the static polarizability along the long axis (81.69 au vs 78.31 au at the HF/6-31(d,p) level), the dynamic field produces a larger effect both for the polarization of individual π bonds (0.665 vs 0.637 and 0.611 vs 0.577 electron) and for the charge transfer (0.357 vs 0.321 electron).

For the pulsed field, the nonadiabatic behavior after the field is turned off is more noticeable for butadiene than for ethylene

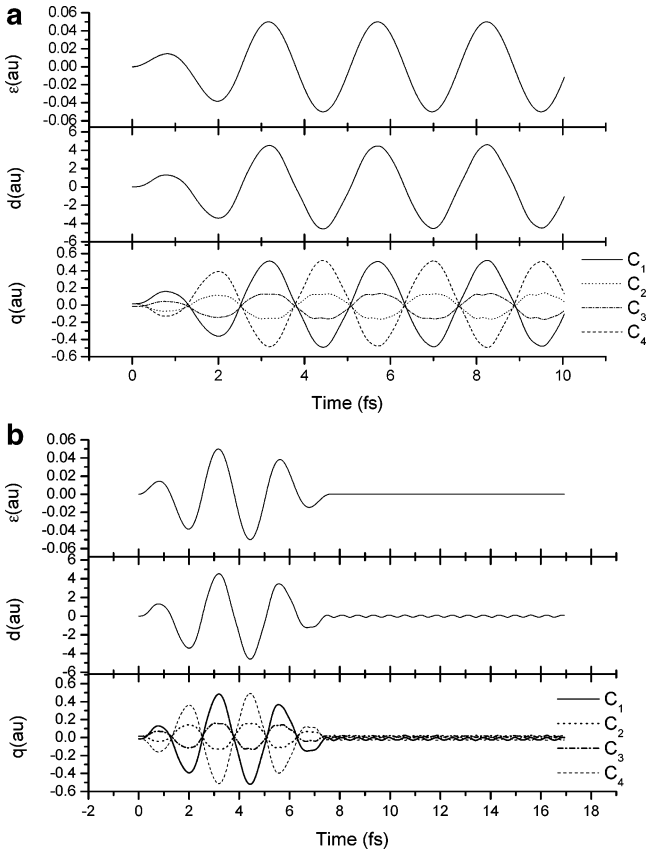

Figure 4. Time evolution of the electric field, instantaneous dipole, and charge distribution of butadiene in CW and pulsed fields (TDHF/6-31G(d,p), $\mathbf{E}_{max} = 0.05$ au (3.5×10^{14} W/cm^2) and $\omega = 0.06$ au (760 nm)).

TABLE 2: Lowest Four Excited States of Butadiene with Oscillator Strength Greater than 0.01 Computed with Linearized TDHF/6-31G(d,p)

excited states	electron transitions (coefficients)	excitation energy in eV (wavelength in nm)	oscillator strength
1^1A_u	HOMO → LUMO (0.65)	6.6040 (187.74)	0.8879
8^1A_u	HOMO−1 → LUMO+1 (0.67)	12.3736 (100.20)	0.1194
	HOMO → LUMO (0.11)		
10^1A_u	HOMO−5 → LUMO+2 (−0.11)	13.6713 (89.27)	0.1774
	HOMO−3 → LUMO+3 (−0.33)		
	HOMO−2 → LUMO+2 (−0.29)		
	HOMO−2 → LUMO+4 (0.47)		
	HOMO−2 → LUMO+6 (0.15)		
11^1A_u	HOMO−3 → LUMO+3 (−0.16)	14.2669 (86.90)	1.0448
	HOMO−3 → LUMO+5 (0.17)		
	HOMO−2 → LUMO+2 (0.59)		
	HOMO−2 → LUMO+4 (0.21)		

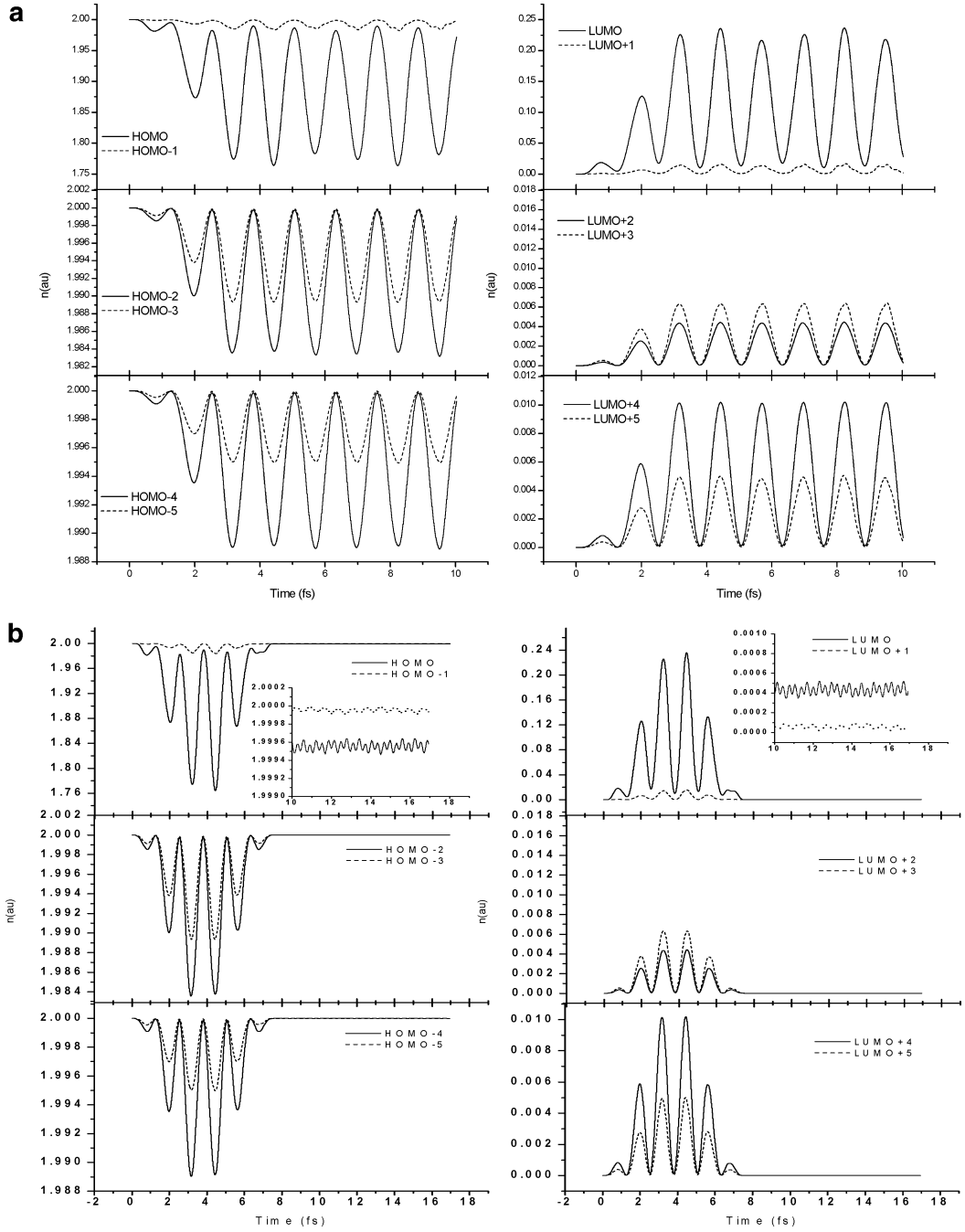

Figure 5. Time evolution of the electron population of the frontier orbitals of butadiene in CW and pulsed fields (TDHF/6-31G(d,p), $\mathbf{E}_{max} = 0.05$ au (3.5×10^{14} W/cm^2) and $\omega = 0.06$ au (760 nm)).

after the field is turned off (compare the magnitudes of the ripples in Figures 2b and 4b). The frequency of the major component of the oscillation is ca. 1.6×10^{15} s^{-1} or ca. 6.6 eV. Table 2 lists the lowest excited states of butadiene. It is apparent that the oscillations in the instantaneous dipole after the field returns to zero correspond to the lowest $\pi \rightarrow \pi^*$ transition at 6.60 eV.

In addition to the two low-lying $\pi \rightarrow \pi^*$ transitions (HOMO $\rightarrow$ LUMO at 6.60 eV and HOMO$-1 \rightarrow$ LUMO$+1$ at 12.37 eV), butadiene has a number of low-lying $\sigma \rightarrow \sigma^*$ transitions with significant intensity. As indicated in Table 2, these transitions involve HOMO-2 to -5 and LUMO$+2$ to $+6$, which are various combinations of C$-$H σ and σ^* orbitals, respectively. Panels a and b in Figure 5 show the evolution of the electronic distribution in terms of the occupation numbers of the six highest occupied and six lowest unoccupied MOs of the field-free ground state for the CW and pulsed fields, respectively. Although the occupation number follows the field mostly adiabatically, some nonadiabatic behavior is noticeable for the HOMO and the LUMO after the first two cycles. This suggests that at the present field strength the coupling is still close to the perturbative regime. As anticipated, the changes in the HOMO and LUMO populations are the largest and correspond to the $1^1A_g \leftrightarrow 1^1A_u$ excitation and relaxation. The intensity of the HOMO$-1 \leftrightarrow$ LUMO$+1$ transition is considerably weaker than the HOMO $\leftrightarrow$ LUMO transition and, hence, the changes in the populations of HOMO-1 and LUMO$+1$ are significantly smaller. The responses of some of the σ and σ^* orbitals are comparable to that of HOMO-1 and LUMO$+1$, since some of these transitions between the σ orbitals have intensities comparable to the HOMO $\leftrightarrow$ LUMO transition.

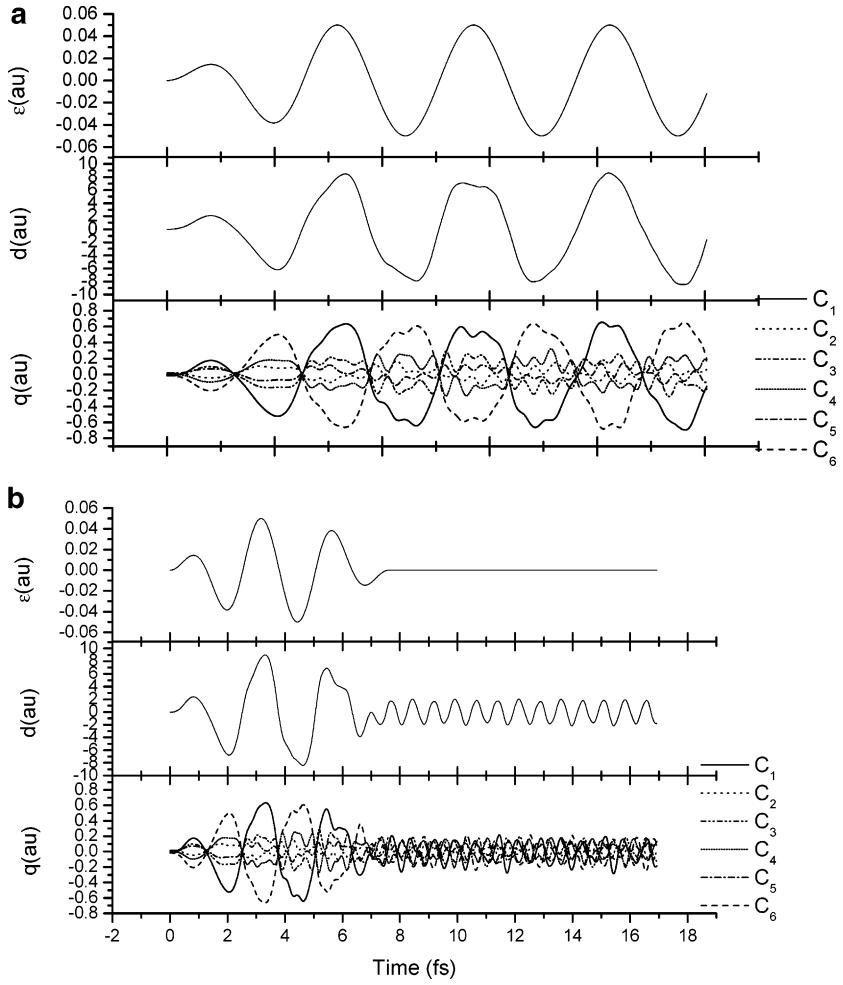

Figure 6. Time evolution of the electric field, instantaneous dipole, and charge distribution of hexatriene in CW and pulsed fields (TDHF/6-31G(d,p), $\mathbf{E}_{max} = 0.05$ au (3.5×10^{14} W/cm^2) and $\omega = 0.06$ au (760 nm)).

As seen in Figure 4b, the instantaneous dipole moment continues to oscillate after the pulsed field returns to zero. The insets in Figure 5b provide a closer look at the populations of the HOMO and LUMO after the pulse has passed. The population of the HOMO has decreased by a small amount and the population of the LUMO has increased by a similar amount (the small oscillations in the HOMO and LUMO population are out-of-phase with each other). This corresponds to a nonadiabatic HOMO → LUMO excitation. Changes in the populations of the other orbitals are smaller by an order of magnitude or more, indicating little or no excitation to higher states.

C. Hexatriene. The response of the dipole and charge distribution of hexatriene to the CW and pulsed fields is shown in Figure 6, panels a and b, respectively. The nonadiabatic behavior of the instantaneous dipole and the charges is readily apparent. In the TDHF simulations with the CW field in Figure 6a, the instantaneous dipole has a maximum magnitude of ca. 9.0 au. Using only the dynamic polarizability, the dipole moment calculated by eq 17 is 8.167 au. This is 9.3% low, compared to only 2.1% low for butadiene and 0.43% low for ethylene. This indicates that the contributions from γ and higher polarizabilities in eq 17 are much more important for hexatriene than for butadiene and ethylene. Thus, as expected, higher order contributions increase nonlinearly as the length and conjugation increase. For the pulsed field shown in Figure 6b, the instantaneous dipole continues to oscillate after the field is turned off. As will be seen below, this corresponds to excitation of the lowest $\pi \rightarrow \pi^*$ transition.

TABLE 3: Lowest Four Excited States of Hexatriene with Oscillator Strength Greater than 0.01 Computed with Linearized TDHF/6-31G(d,p)

excited states	electron transitions (coefficients)	excitation energy in eV (wavelength in nm)	oscillator strength
1^1A	HOMO → LUMO (0.68)	5.6464 (219.58)	1.3611
	HOMO−1 → LUMO+1 (0.12)		
7^1A	HOMO−2 → LUMO (0.46)	8.9922 (137.88)	0.0533
	HOMO−1 → LUMO+1 (−0.28)		
	HOMO → LUMO+5 (−0.41)		
18^1A	HOMO−2 → LUMO (−0.18)	11.5099 (107.72)	0.1632
	HOMO−2 → LUMO+5 (0.33)		
	HOMO−1 → LUMO+1 (0.54)		
	HOMO → LUMO (−0.14)		
	HOMO → LUMO+5 (−0.16)		
29^1A	HOMO−7 → LUMO+4 (0.10)	13.7274 (90.32)	0.2924
	HOMO−6 → LUMO+3 (0.12)		
	HOMO−5 → LUMO+3 (0.12)		
	HOMO−4 → LUMO+4 (−0.33)		
	HOMO−4 → LUMO+7 (0.13)		
	HOMO−3 → LUMO+1 (0.36)		
	HOMO−3 → LUMO+2 (0.36)		

The static external field of 0.05 au directed along the long axis of hexatriene induces charges of 0.5814, −0.0593, 0.1813, −0.1596, 0.0685, and −0.6123 on C_1 to C_6, respectively (Figure 1). As in butadiene, this can be understood in terms of polarization within localized π bonds and charge transfer between π bonds. While the polarization within the terminal π bonds is similar to that of butadiene, the charge transfer between

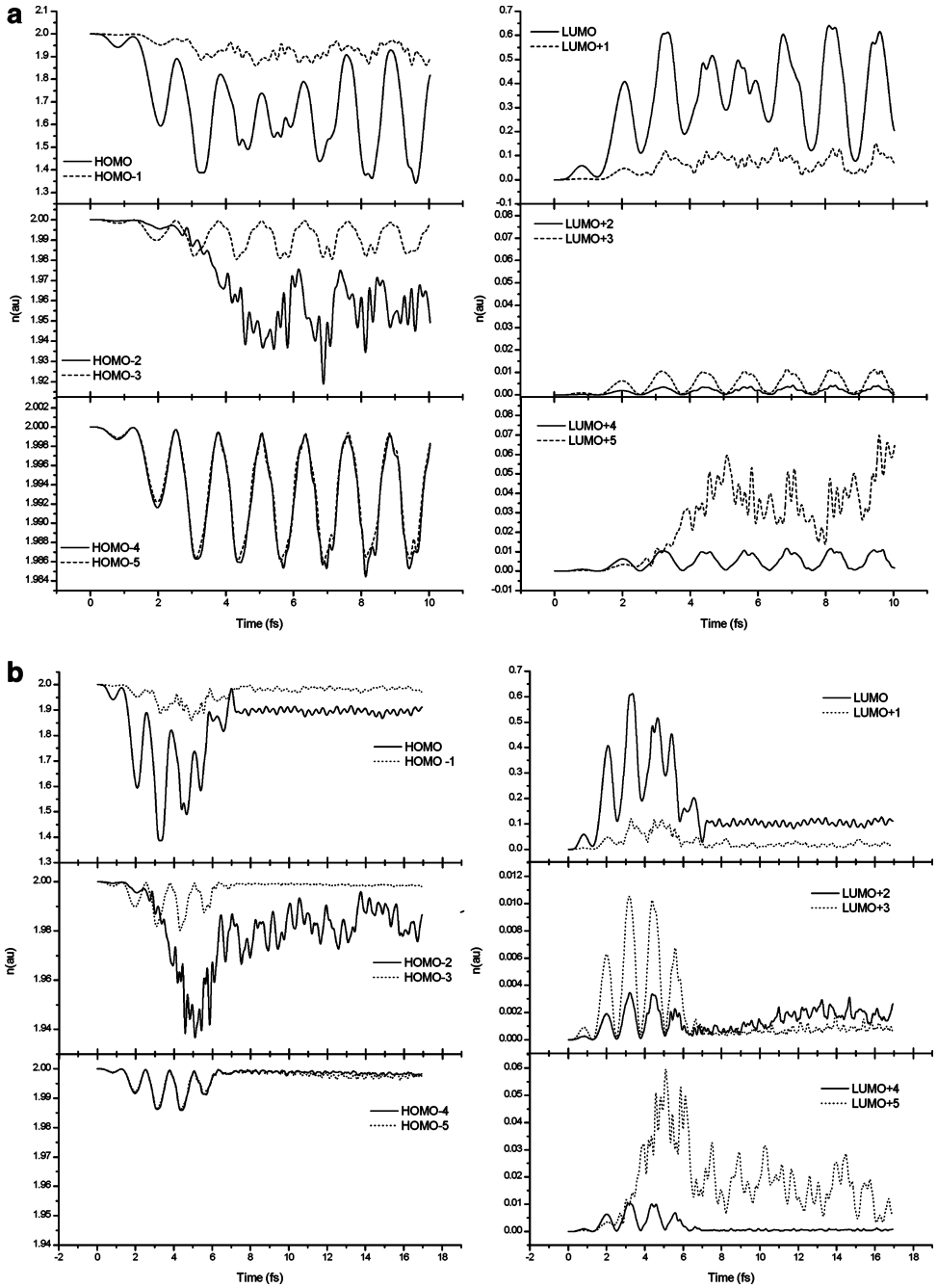

Figure 7. Time evolution of the electron population of the frontier orbitals of hexatriene in CW and pulsed fields (TDHF/6-31G(d,p), $\mathbf{E}_{max} = 0.05$ au (3.5×10^{14} W/cm^2) and $\omega = 0.06$ au (760 nm)).

these π bonds is considerably larger than that in butadiene (ca. 0.66 vs 0.32 electron). A simple Hückel model gives the same trend in charges and reproduces the smaller polarization seen in the central π bond.

For hexatriene with a CW field in the longitudinal direction, the time evolution of the charge distribution becomes rather complicated. The charges on C_1 and C_6 follow the field nonadiabatically, but their average response is still comparable to the field. Charges on C_2, C_3, C_4, and C_5 change sign at the expected points where the field changes sign but exhibit several nonperiodic oscillations before the next change in field sign. In keeping with the response to the static field, the charges on C_3 and C_4 experience larger amplitude oscillations than those on C_2 and C_5. The maximum charge separation in this case is 0.633, −0.01585, 0.173, −0.139, 0.0103, and −0.661 au. The charge transferred between the right and left halves of the molecule behaves somewhat more smoothly than the individual charges. In the static case, the maximum charge transfer between the halves of the molecule is 0.703 electron. In the dynamic case, the charge transfer is considerably larger, 0.790 electron, indicating that dynamic effects significantly enhance the charge separation. The difference in the charge separation due to static and dynamic fields is 0.008, 0.036, and 0.087 electron for ethylene, butadiene, and hexatriene, respectively. Here, again, we observe the nonlinear trend in the strength of the dynamic field coupling with a molecule as the molecular size and conjugation increase. Similar trends have been observed for dynamic polarizability of linear polyenes with increasing molecular length and conjugation.[36−38,40,41,43,44]

The electron distribution in terms of the occupation numbers of the six highest occupied and six lowest unoccupied MOs of the field-free ground state is shown in Figure 7a,b for the CW

and pulsed fields, respectively. HOMO−2 to LUMO+1 and LUMO+5 are the π orbitals and show the largest changes in population and the greatest nonadiabatic behavior. The changes in the populations of the HOMO and LUMO are more than twice as large as those in butadiene and follow the field adiabatically only for the first cycle and a half. The populations of the other π orbitals, HOMO−2, HOMO−1, LUMO+1, and LUMO+5, show a particularly complex time evolution after the first cycle. The second and third $\pi \rightarrow \pi^*$ transitions both involve a combination of these orbitals (see Table 3) and could account for the complex behavior. The changes in the populations of the σ and σ^* orbitals are more nearly adiabatic. Thus, the present field strength produces markedly nonadiabatic behavior in hexatriene while it leads to slight nonadiabatic character for butadiene and no nonadiabatic character for ethylene. As expected, the nonadiabatic character increases with molecular length and increasing conjugation.

For the pulsed field, the oscillation in the dipole after the field is turned off is clearly visible. The frequency of this oscillation is ca. 1.35×10^{15} s^{-1} or ca. 5.6 eV. This corresponds to the lowest $\pi \rightarrow \pi^*$ transition of hexatriene, 5.65 eV (see Table 3). Figure 7b shows that ca. 0.1 electron has been transferred from the HOMO to the LUMO by the short pulse. In addition, about 0.02 electron has been transferred from HOMO−1 and HOMO−2 to LUMO+1 and LUMO+5, and the populations in these orbitals have substantial and comparable fluctuations even after the field returns to zero. Comparison of the behavior of ethylene, butadiene, and hexatriene after the pulsed field shows that the probability for excitation increases quite dramatically with the length of the conjugated system.

These results seem to concur with the analytical model of nonadiabatic excitation of polyatomic molecules known as NMED.[25−28] In the NMED model the strong electric field of the laser causes coupling between the ground and the excited-state manifold. A nonadiabatic electronic transition from the ground state to the excited-state manifold is the first and rate-limiting step in the ionization process. This may be the nonadiabatic $\pi \rightarrow \pi^*$ transition that is observed in these simulations. Although this simple analytical model quantitatively agrees with experimental results on ionization and dissociation on a number of conjugated systems, several assumptions were made that make the analytical model difficult to apply to more than a few molecules of simple shape. In the calculations presented here, these simplifying assumptions did not have to be made. Moreover, this computational method can easily be applied to study the response of molecules of arbitrary shape.

IV. Conclusion

In this paper, we have used TDHF to simulate strong laser fields interacting with a series of polyenes of increasing length and conjugation. Ethylene, butadiene, and hexatriene were examined in the nonionizing regime with the field aligned along the long axis of the molecules. The calculations employed both CW and pulsed fields with an intensity of 8.75×10^{13} W/cm^2 and a wavelength of 760 nm. The time evolution of the charges, instantaneous dipole, and orbital occupations were used to assess the effect of strong fields on these polyenes. Ethylene responds adiabatically. Butadiene begins to show some nonadiabatic effects, while hexatriene displays very pronounced nonadiabatic effects. For the same laser intensity, nonadiabatic effects increase nonlinearly with the length of the polyene. For pulsed fields, the instantaneous dipole continues to oscillate after the field returned to zero. This indicates that nonadiabatic excitation of polyatomic molecules by a nonresonance strong-field laser pulse is possible. For all three molecules studied, the greatest nonresonant electronic excitation was the lowest $\pi \rightarrow \pi^*$ excitation that involves the HOMO to LUMO transition and this response was greatest for hexatriene.

There are numerous questions that can be addressed by using the computational methodology presented here. With the addition of nuclear motion it may be possible to interpret the outcomes of shaped laser pulse molecule interactions in terms of the underlying energy partitioning. This publication is one step in an ongoing effort to create a reliable methodology that will help advance the understanding of laser−molecule interactions.

Acknowledgment. This work was supported by the National Science Foundation (CHE 0131157, H.B.S.; and CHE 313967, R.J.L.) and Gaussian Inc.

References and Notes

(1) Bhardwaj, V. R.; Corkum, P. B.; Rayner, D. M. Internal laser-induced dipole force at work in C-60 molecule. *Phys. Rev. Lett.* **2003**, *91*.

(2) Cornaggia, C.; Lavancier, J.; Normand, D.; Morellec, J.; Agostini, P.; Chambaret, J. P.; Antonetti, A. Multielectron Dissociative Ionization of Diatomic-Molecules in an Intense Femtosecond Laser Field. *Phys. Rev. A* **1991**, *44*, 4499.

(3) Cornaggia, C.; Schmidt, M.; Normand, D. Coulomb Explosion of CO_2 in an Intense Femtosecond Laser Field. *J. Phys. B* **1994**, *27*, L123.

(4) Markevitch, A. N.; Romanov, D. A.; Smith, S. M.; Levis, R. J. Coulomb explosion of large polyatomic molecules assisted by nonadiabatic charge localization. *Phys. Rev. Lett.* **2004**, *92*.

(5) Muller, H. G.; Bucksbaum, P. H.; Schumacher, D. W.; Zavriyev, A. Above-Threshold Ionization with a 2-Color Laser Field. *J. Phys. B* **1990**, *23*, 2761.

(6) Eberly, J. H.; Javanainen, J.; Rzazewski, K. Above-Threshold Ionization. *Phys. Rep.* **1991**, *204*, 331.

(7) Graham, P.; Menkir, G.; Levis, R. J. An investigation of the effects of experimental parameters on the closed-loop control of photoionization/dissociation processes in acetophenone. *Spec. Chim. Acta B* **2003**, *58*, 1097.

(8) Levis, R. J.; Rabitz, H. A. Closing the loop on bond selective chemistry using tailored strong field laser pulses. *J. Phys. Chem. A* **2002**, *106*, 6427.

(9) Markevitch, A. N.; Moore, N. P.; Levis, R. J. The effects of molecular structure on strong field energy coupling of anthracene and anthraquinone. *Abstr. Pap. Am. Chem. Soc.* **2001**, *221*, U294.

(10) Levis, R. J.; Menkir, G. M.; Rabitz, H. Selective bond dissociation and rearrangement with optimally tailored, strong-field laser pulses. *Science* **2001**, *292*, 709.

(11) Levis, R. J.; DeWitt, M. J. Photoexcitation, ionization, and dissociation of molecules using intense near-infrared radiation of femtosecond duration. *J. Phys. Chem. A* **1999**, *103*, 6493.

(12) DeWitt, M. J.; Peters, D. W.; Levis, R. J. Photoionization/dissociation of alkyl substituted benzene molecules using intense near-infrared radiation. *Chem. Phys.* **1997**, *218*, 211.

(13) Dewitt, M. J.; Levis, R. J. Near-Infrared Femtosecond Photoionization Dissociation of Cyclic Aromatic-Hydrocarbons. *J. Chem. Phys.* **1995**, *102*, 8670.

(14) McPherson, A.; Gibson, G.; Jara, H.; Johann, U.; Luk, T. S.; McIntyre, I. A.; Boyer, K.; Rhodes, C. K. Studies of Multiphoton Production of Vacuum Ultraviolet-Radiation in the Rare-Gases. *J. Opt. Soc. Am.* **1987**, *4*, 595.

(15) Zuo, T.; Bandrauk, A. D. High-Order Harmonic-Generation in Intense Laser and Magnetic-Fields. *J. Nonlin. Opt. Phys. Mater.* **1995**, *4*, 533.

(16) Lhuillier, A.; Schafer, K. J.; Kulander, K. C. Theoretical Aspects of Intense Field Harmonic-Generation. *J. Phys. B* **1991**, *24*, 3315.

(17) Antoine, P.; Lhuillier, A.; Lewenstein, M. Attosecond pulse trains using high-order harmonics. *Phys. Rev. Lett.* **1996**, *77*, 1234.

(18) Salieres, P.; Antoine, P.; de Bohan, A.; Lewenstein, M. Temporal and spectral tailoring of high-order harmonics. *Phys. Rev. Lett.* **1998**, *81*, 5544.

(19) Suzuki, M.; Mukamel, S. Charge and bonding redistribution in octatetraene driven by a strong laser field: Time-dependent Hartree−Fock simulation. *J. Chem. Phys.* **2003**, *119*, 4722.

(20) Bucksbaum, P. H.; Zavriyev, A.; Muller, H. G.; Schumacher, D. W. Softening of the H2+ Molecular-Bond in Intense Laser Fields. *Phys. Rev. Lett.* **1990**, *64*, 1883.

(21) Zavriyev, A.; Bucksbaum, P. H.; Muller, H. G.; Schumacher, D. W. Ionization and Dissociation of H2 in Intense Laser Fields at 1.064-Mu-M, 532 Nm, and 355-Nm. *Phys. Rev. A* **1990**, *42*, 5500.

(22) Frasinski, L. J.; Posthumus, J. H.; Plumridge, J.; Codling, K.; Taday, P. F.; Langley, A. J. Manipulation of bond hardening in H-2(+) by chirping of intense femtosecond laser pulses. *Phys. Rev. Lett.* **1999**, *83*, 3625.

(23) Zuo, T.; Bandrauk, A. D. Charge-Resonance-Enhanced Ionization of Diatomic Molecular-Ions by Intense Lasers. *Phys. Rev. A* **1995**, *52*, R2511.

(24) Seideman, T.; Ivanov, M. Y.; Corkum, P. B. Role of Electron Localization in Intense-Field Molecular Ionization. *Phys. Rev. Lett.* **1995**, *75*, 2819.

(25) Lezius, M.; Blanchet, V.; Rayner, D. M.; Villeneuve, D. M.; Stolow, A.; Ivanov, M. Y. Nonadiabatic multielectron dynamics in strong field molecular ionization. *Phys. Rev. Lett.* **2001**, *86*, 51.

(26) Lezius, M.; Blanchet, V.; Ivanov, M. Y.; Stolow, A. Polyatomic molecules in strong laser fields: Nonadiabatic multielectron dynamics. *J. Chem. Phys.* **2002**, *117*, 1575.

(27) Markevitch, A. N.; Smith, S. M.; Romanov, D. A.; Schlegel, H. B.; Ivanov, M. Y.; Levis, R. J. Nonadiabatic dynamics of polyatomic molecules and ions in strong laser fields. *Phys. Rev. A* **2003**, *68*, 011402(R).

(28) Markevitch, A. N.; Romanov, D. A.; Smith, S. M.; Schlegel, H. B.; Ivanov, M. Y.; Levis, R. J. Sequential nonadiabatic excitation of large molecules and ions driven by strong laser fields. *Phys. Rev. A* **2004**, *69*, 013401.

(29) Markevitch, A. N.; Moore, N. P.; Levis, R. J. The influence of molecular structure on strong field energy coupling and partitioning. *Chem. Phys.* **2001**, *267*, 131.

(30) DeWitt, M. J.; Levis, R. J. Observing the transition from a multiphoton-dominated to a field-mediated ionization process for polyatomic molecules in intense laser fields. *Phys. Rev. Lett.* **1998**, *81*, 5101.

(31) DeWitt, M. J.; Levis, R. J. Calculating the Keldysh adiabaticity parameter for atomic, diatomic, and polyatomic molecules. *J. Chem. Phys.* **1998**, *108*, 7739.

(32) DeWitt, M. J.; Levis, R. J. Concerning the ionization of large polyatomic molecules with intense ultrafast lasers. *J. Chem. Phys.* **1999**, *110*, 11368.

(33) Tchaplyguine, M.; Hoffmann, K.; Duhr, O.; Hohmann, H.; Korn, G.; Rottke, H.; Wittmann, M.; Hertel, I. V.; Campbell, E. E. B. Ionization and fragmentation of C-60 with sub-50 fs laser pulses. *J. Chem. Phys.* **2000**, *112*, 2781.

(34) von Helden, G.; Holleman, I.; Knippels, G. M. H.; van der Meer, A. F. G.; Meijer, G. Infrared resonance enhanced multiphoton ionization of fullerenes. *Phys. Rev. Lett.* **1997**, *79*, 5234.

(35) Muth-Bohm, J.; Becker, A.; Chin, S. L.; Faisal, F. H. M. S-matrix theory of ionisation of polyatomic molecules in an intense laser pulse. *Chem. Phys. Lett.* **2001**, *337*, 313.

(36) Oliveira, L. N.; Amaral, O. A. V.; Castro, M. A.; Fonseca, T. L. Static polarizabilities of doubly charged polyacetylene oligomers: basis set and electron correlation effects. *Chem. Phys.* **2003**, *289*, 221.

(37) Schulz, M.; Tretiak, S.; Chernyak, V.; Mukamel, S. Size scaling of third-order off-resonant polarizabilities. Electronic coherence in organic oligomers. *J. Am. Chem. Soc.* **2000**, *122*, 452.

(38) Tretiak, S.; Chernyak, V.; Mukamel, S. Chemical bonding and size scaling of nonlinear polarizabilities of conjugated polymers. *Phys. Rev. Lett.* **1996**, *77*, 4656.

(39) Meier, T.; Mukamel, S. Femtosecond spectroscopic signatures of electronic correlations in conjugated polyenes and semiconductor nanostructures. *Phys. Rev. Lett.* **1996**, *77*, 3471.

(40) Tretiak, S.; Chernyak, V.; Mukamel, S. Collective electronic oscillators for nonlinear optical response of conjugated molecules. *Chem. Phys. Lett.* **1996**, *259*, 55.

(41) Shanker, B.; Applequist, J. Atom monopole-dipole interaction model with limited delocalization length for polarizabilities of polyenes. *J. Phys. Chem.* **1996**, *100*, 10834.

(42) Chen, G. H.; Mukamel, S. Nonlinear Polarizabilities of donor−acceptor substituted conjugated polyenes. *J. Phys. Chem.* **1996**, *100*, 11080.

(43) Kirtman, B.; Toto, J. L.; Robins, K. A.; Hasan, M. Ab-Initio Finite Oligomer Method for Nonlinear-Optical Properties of Conjugated Polymers, Hartree−Fock Static Longitudinal Hyperpolarizability of Polyacetylene. *J. Chem. Phys.* **1995**, *102*, 5350.

(44) Smith, S. M.; Markevitch, A. N.; Romanov, D. A.; Li, X. S.; Levis, R. J.; Schlegel, H. B. Static and dynamic polarizabilities of conjugated molecules and their cations. *J. Phys. Chem. A* **2004**, *108*, 11063.

(45) Ingamells, V. E.; Papadopoulos, M. G.; Raptis, S. G. Vibrational effects on the polarizability and second hyperpolarizability of ethylene. *Chem. Phys. Lett.* **1999**, *307*, 484.

(46) Rozyczko, P. B.; Bartlett, R. J. The hyperpolarizability of *trans*-butadiene rerevisited. *J. Chem. Phys.* **1998**, *108*, 7988.

(47) Bandrauk, A. D. In *Molecules in Laser Fields*; M. Dekker: New York, 1993.

(48) *Atomic and Molecular Processes with Short Intense Laser Pulses*; Bandrauk, A. D., Ed.; NATO ASI B171; Plenum Press: 1988.

(49) *Coherence Phenomena in Atoms and Molecules in Laser Fields*; Bandrauk, A. D.; Wallace, S. C., Eds.; NATO ASI B278, Plenum Press: New York, 1992.

(50) Muller, H. G. Tunneling excitation to resonant states in helium as main source of superponderomotive photoelectrons in the tunneling regime. *Phys. Rev. Lett.* **1999**, *83*, 3158.

(51) Nandor, M. J.; Walker, M. A.; Van Woerkom, L. D.; Muller, H. G. Detailed comparison of above-threshold-ionization spectra from accurate numerical integrations and high-resolution measurements. *Phys. Rev. A* **1999**, *60*, R1771.

(52) Muller, H. G. Numerical simulation of high-order above-threshold-ionization enhancement in argon. *Phys. Rev. A* **1999**, *60*, 1341.

(53) Lein, M.; Kreibich, T.; Gross, E. K. U.; Engel, V. Strong-field ionization dynamics of a model H-2 molecule. *Phys. Rev. A* **2002**, *65*.

(54) Kulander, K. C. Time-Dependent Hartree−Fock Theory of Multiphoton Ionization−Helium. *Phys. Rev. A* **1987**, *36*, 2726.

(55) Kulander, K. C. Multiphoton Ionization of Hydrogen−a Time-Dependent Theory. *Phys. Rev. A* **1987**, *35*, 445.

(56) Tsiper, E. V.; Chernyak, V.; Tretiak, S.; Mukamel, S. Ground-state density-matrix algorithm for excited-state adiabatic surfaces: application to polyenes. *Chem. Phys. Lett.* **1999**, *302*, 77.

(57) Micha, D. A. Time-evolution of multiconfiguration density functions driven by nuclear motions. *Int. J. Quantum Chem.* **1996**, *60*, 109.

(58) Li, X. S.; Smith, S. M.; Markevitch, A. N.; Romanov, D. A.; Levis, R. J.; Schlegel, H. B. A time-dependent Hartree−Fock approach for studying the electronic optical response of molecules in intense fields. *Phys. Chem. Chem. Phys.* **2005**, *7*, 233.

(59) Suzuki, M.; Mukamel, S. Many-body effects in molecular photoionization in intense laser fields; time-dependent Hartree−Fock simulations. *J. Chem. Phys.* **2004**, *120*, 669.

(60) Hankin, S. M.; Villeneuve, D. M.; Corkum, P. B.; Rayner, D. M. Nonlinear ionization of organic molecules in high-intensity laser fields. *Phys. Rev. Lett.* **2000**, *84*, 5082.

(61) Hankin, S. M.; Villeneuve, D. M.; Corkum, P. B.; Rayner, D. M. Intense-field laser ionization rates in atoms and molecules. *Phys. Rev. A* **2001**, *6401*, art. no. 013405.

(62) Micha, D. A. Time-dependent many-electron treatment of electronic energy and charge transfer in atomic collisions. *J. Phys. Chem. A* **1999**, *103*, 7562.

(63) Micha, D. A. Density matrix treatment of electronic rearrangement. In *Adva. Quantum Chem.* **1999**, *35*, 317.

(64) Development version of GAUSSIAN series of programs: Frisch, M. J.; Trucks, G. W.; Schlegel, H. B.; Scuseria, G. E.; Robb, M. A.; Cheeseman, J. R.; Montgomery, J. A., Jr.; Vreven, T.; Kudin, K. N.; Burant, J. C.; Millam, J. M.; Iyengar, S. S.; Tomasi, J.; Barone, V.; Mennucci, B.; Cossi, M.; Scalmani, G.; Rega, N.; Petersson, G. A.; Nakatsuji, H.; Hada, M.; Ehara, M.; Toyota, K.; Fukuda, R.; Hasegawa, J.; Ishida, M.; Nakajima, T.; Honda, Y.; Kitao, O.; Nakai, H.; Klene, M.; Li, X.; Knox, J. E.; Hratchian, H. P.; Cross, J. B.; Bakken, V.; Adamo, C.; Jaramillo, J.; Gomperts, R.; Stratmann, R. E.; Yazyev, O.; Austin, A. J.; Cammi, R.; Pomelli, C.; Ochterski, J. W.; Ayala, P. Y.; Morokuma, K.; Voth, G. A.; Salvador, P.; Dannenberg, J. J.; Zakrzewski, V. G.; Dapprich, S.; Daniels, A. D.; Strain, M. C.; Farkas, O.; Malick, D. K.; Rabuck, A. D.; Raghavachari, K.; Foresman, J. B.; Ortiz, J. V.; Cui, Q.; Baboul, A. G.; Clifford, S.; Cioslowski, J.; Stefanov, B. B.; Liu, G.; Liashenko, A.; Piskorz, P.; Komaromi, I.; Martin, R. L.; Fox, D. J.; Keith, T.; Al-Laham, M. A.; Peng, C. Y.; Nanayakkara, A.; Challacombe, M.; Gill, P. M. W.; Johnson, B.; Chen, W.; Wong, M. W.; Gonzalez, C.; Pople, J. A. Gaussian, Inc.: Wallingford, CT, 2004.

(65) Hansen, A. E.; Bouman, T. D. Natural chiroptical spectroscopy: theory and computations. *Adv. Chem. Phys.* **1980**, *44*, 545.

(66) Hansen, A. E.; Voigt, B.; Rettrup, S.; Bouman, T. D. Large-Scale RPA Calculations of Chiroptical Properties of Organic-Molecules−Program RPAC. *Int. J. Quantum Chem.* **1983**, *23*, 595.

(67) Oddershede, J. Polarization propagator calculations. *Adv. Quantum Chem.* **1978**, *11*, 275.